aerospace

MDPI

Article

Retrospective Analysis of Pulse Wave Flattening for G-LOC Detection Using Automatic Computer Algorithm Methods

Janina Sammito [1,2], Anthony Schwarz [1], Michael Nehring [1] and Stefan Sammito [1,2,*]

[1] German Air Force Centre of Aerospace Medicine, 51147 Cologne, Germany
[2] Occupational Medicine, Faculty of Medicine, Otto-von-Guericke-University of Magdeburg, 39106 Magdeburg, Germany
* Correspondence: stefansammito@bundeswehr.org; Tel.: +49-2203-9863-1320

Abstract

The possibility of G-induced loss of consciousness (G-LOC) is a key concern when flying modern, high-performance aircraft. Currently, there are no identification methods available based on physiological data. This study aimed to determine whether specific pulse wave changes could be reliably identified using automatic computer algorithms to detect impending G-LOC. The pulse waves of 86 people who experienced G-LOC in a human centrifuge were analysed alongside an age-, gender-, nationality-, training-, and anti-G-equipment-matched control group using computer algorithm methods to analyse possible longer reductions in the G-LOC group. Based on this data, the study showed that centrifuge profiles with a gradual "onset run" using AGSM resulted in longer pulse wave flattening around the G-LOC in the G-LOC group than in the matched control group. However, this could not be verified in human centrifuge runs with active flight profiles and higher onset rates. Unfortunately, this means that the method used here would not currently be applicable in actual flight. In the future, the possibility of creating an identification method could be extended by incorporating additional physiological data.

Keywords: high-performance aircraft; military; aviator; high G; gravitation; pilot

1. Introduction

The continuous development of military aircraft since World War I has led to the emergence of modern high-performance aircraft (HPA) of the so-called 4th and 5th generations, which are now an integral part of numerous air forces. They are characterised by high acceleration rates and complex flight manoeuvres, which are accompanied by high $+G_z$ loads. The manoeuvrability of these military aircraft, which can be flown beyond the limits of human acceleration tolerance [1], regularly pushes pilots to the limits of their physiological endurance [2,3].

Among other things, high $+G_z$ forces affect the pulmonary system and the cardiovascular system [2]; there is a redistribution of blood and other bodily fluids [4], which can lead to cerebral hypoperfusion [3,5,6]. If the stress caused by the $+G_z$ forces exceeds the individual G tolerance, the reduced perfusion of the eyes leads to a loss of colour vision, known as grey-out, and tunnel vision, whereas reduced cerebral perfusion can lead to an "almost loss of consciousness" (A-LOC) [1]. A-LOC severely impairs pilots' cognitive, motor and emotional responses [7,8] and can sometimes lead to memory lapses and reduced control over muscle function [7]. There is only a fine line between A-LOC and

Check for updates

Academic Editor: Miroslav Kelemen

Received: 3 March 2026
Revised: 22 April 2026
Accepted: 24 April 2026
Published: 27 April 2026

Copyright: © 2026 by the authors. Licensee MDPI, Basel, Switzerland. This article is an open access article distributed under the terms and conditions of the Creative Commons Attribution (CC BY) license.

complete unconsciousness caused by oxygen deprivation [4–6], known as G-induced loss of consciousness (G-LOC) [7].

G-LOC poses a danger to pilots due to the complete inability to act caused by loss of consciousness [4,9–12]. The average duration of complete incapacitation in a G-LOC is stated as 12 s [13]. It can take anywhere from 12 s to 2–3 min for pilots to fully recover from G-LOC before they are able to actively take control of the aircraft again [10,14,15]. Therefore, G-LOC can pose a significant threat to flight safety through so-called "mishaps", which in the worst case can result in the loss of human life and aircraft [14,16].

There are a number of countermeasures, all of which aim to maintain sufficient cerebral blood flow under $+G_z$ stress and strengthen G tolerance [5,17,18]. This includes the specific design of the ejection seat in relation to the seat back angle, as well as special anti-G suits, positive pressure breathing for G protection (PBG) and the anti-G straining manoeuvre (AGSM) [5,17,18]. These countermeasures are capable of reducing the above-mentioned G-LOC hazards, but they cannot eliminate them completely [17]. There are also a number of measurement methods in centrifuge training and research that record the physiological condition of pilots under G-force stress and are designed to identify changes that could cause G-LOC in particular [9,17]. These include electromyography (EMG), electrocardiography (ECG), electroencephalography (EEG) and near-infrared spectroscopy (NIRS) [2,4,7,17].

The occurrence of G-LOC is complex, and to date there are no known valid physiological measurement methods that can be used in flight to clearly identify the occurrence of G-LOC shortly before or during G-LOC based on changes in vital parameter values [2,4,8,9,11,12,19,20].

The aim of this research project was therefore to determine whether specific pulse wave changes can be reliably identified using automatic computer algorithms in order to detect an impending G-LOC in advance.

2. Materials and Methods

A retrospective data analysis was performed on the recorded physiological monitoring, video recordings and technical data of all course participants who suffered G-LOC during human centrifuge training between 1 January 2013 and 15 September 2023. The centrifuge training was conducted using the high-G human centrifuge at the German Air Force Centre of Aerospace Medicine (GAFCAM) in Königsbrück, Germany, manufactured by AMST (Ranshofen, Austria, built in 1986), which allows G-forces of up to $+15\ G_z$ with a maximum on and offset of 10 G/s (see Figure 1).

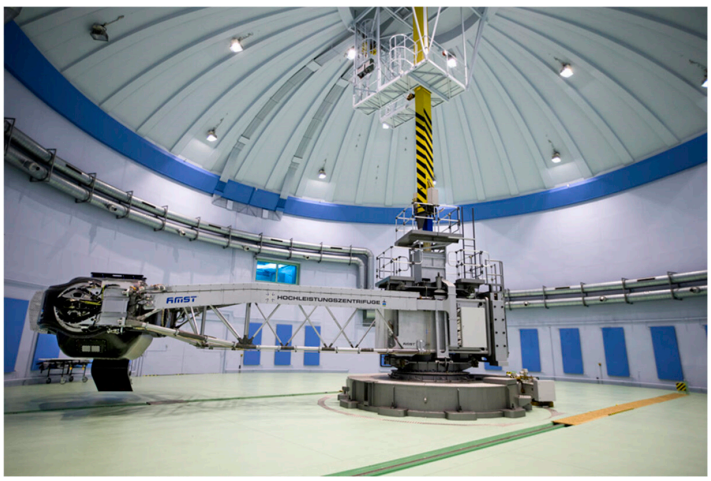


Figure 1. The human centrifuge at the Aviation Physiology Training Centre of the German Air Force Centre of Aerospace Medicine in Königsbrück, on 14 January 2020 (image source: German Armed Forces/Torsten Kraatz).

In total, human centrifuge training was provided for 2830 course participants during the above-mentioned period, with a total of 7175 human centrifuge runs. The training participants completed different G-profiles (see Figure 2) in the human centrifuge in a specified order.

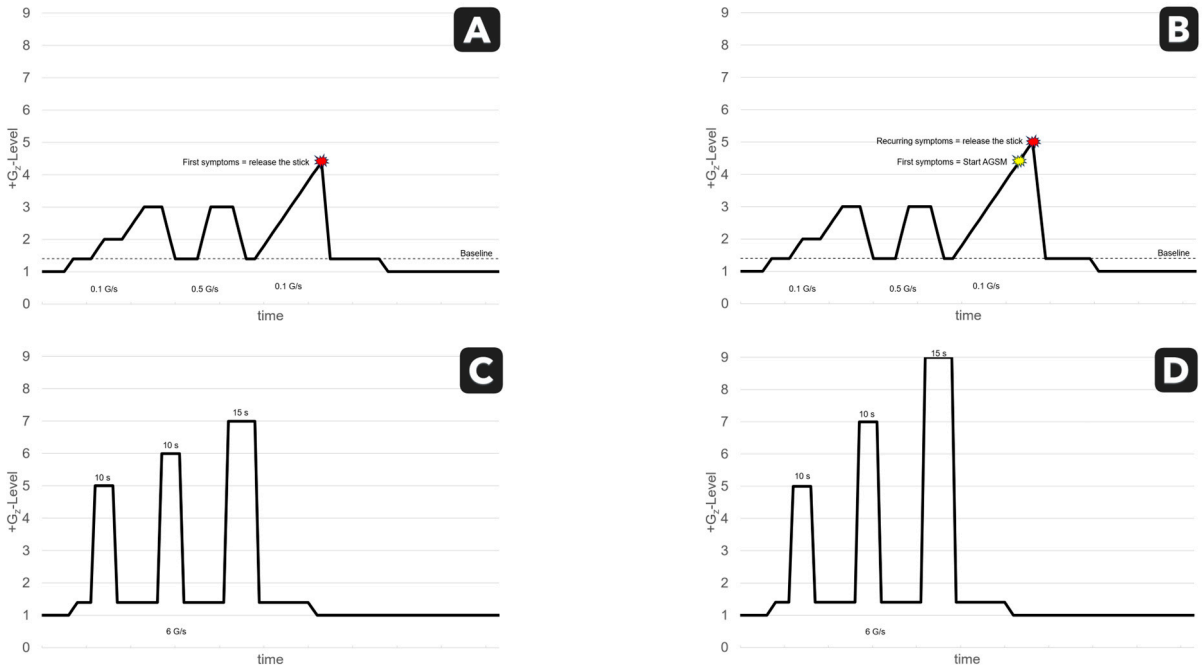


Figure 2. Acclimatisation profile and linear profile (**A**) without and (**B**) with anti-G straining manoeuvre (AGSM); (**C**) example of human centrifuge profile with anti-G trousers (Active I); (**D**) example of human centrifuge profile with complete Full Coverage Anti-G suit (Active II).

First, a standardised acclimatisation profile (AP) was carried out, followed immediately by a linear profile (LP) (see Figure 2A). The aim of this human centrifuge run is to enable participants to become accustomed to the human centrifuge at low $+G_z$ loads in the AP and to recognise individual visual symptoms when natural G tolerance is reached in the LP. The profile is completed without anti-G equipment and AGSM. A preset profile is completed automatically, which means that the pilot has no influence on the maximum $+G_z$ load and the on and offset. Only at the end of the AP, during the transition to LP, must a button on the back of the control stick be pressed and held, which the pilot should release as soon as the first visual symptoms due to the $+G_z$ load appear. When the button is released, the human centrifuge stops automatically and immediately with an offset of 1.5 G/s until a load of +2.5 G_z is reached, and then with reduced deceleration of 0.5 G/s until the human centrifuge comes to a complete stop.

As an alternative to this AP + LP, there were deviations due to national requirements, whereby the AGSM was performed in the LP after reaching the natural G tolerance with initial visual symptoms. With further acceleration and continuation of the AGSM, at an onset of 0.1 G/s, the centrifuge was stopped by releasing the control button mentioned above as soon as visual symptoms reappeared (see Figure 2B).

Subsequently, prospective or active pilots underwent a second human centrifuge run with higher G-forces, using anti-G equipment. Starting from a baseline of +1.4 G_z, course participants were able to independently control a predefined $+G_z$ maximum as well as the on and offset of the $+G_z$ load (max. 6 G/s) by actively pulling or releasing the control stick. When using only the anti-G trousers (five bladder configuration: left and right calf, left and right thigh, abdominal), normally the maximum G-load was +7 G_z, and the AGSM was performed with guidance via microphone (Active I, see Figure 2C). With a Full Coverage

Anti-G suit, the maximum G-load was +9 G_z. Depending on the respective nationality of the pilots, the profiles differed slightly in terms of maximum +G_z stress and time under +G_z stress (Active II, see Figure 2D). During the centrifuge run, participants were required to hold the "dead man's switch" on the joystick. In the event of a G-LOC, participants would typically lose control of this position, and releasing the joystick would automatically trigger the gongela to decelerate at a rate of 6 G/s. If a participant experienced a G-LOC but this did not result in the run being automatically terminated, the responsible flight surgeon in the control room could stop the centrifuge centrally with a deceleration of 6 G/s based on video footage and in the absence of a verbal response from the participant.

All test subjects were monitored during the centrifuge runs using a 1-channel ECG (g.tec GmbH, Schiedlberg, Austria) to record their heart rate and pulse wave using an ear clip (model 8000Q2, Nonin Medical, Inc., Plymouth, MN, USA) with a measuring wavelength of 660 nm (measurement of deoxygenated haemoglobin) and 910 nm (measurement of oxygenated haemoglobin) or a forehead sensor (model 8000R, Nonin Medical, Inc., Plymouth, MN, USA) when using a Full Coverage Anti-G suit. Video monitoring and audio connection were also used to assess the test subjects.

All participants were required to have a valid aviation medical certificate or an internationally comparable medical examination equivalent to this in order to take part in the course. In addition, a further medical examination was carried out prior to participation, along with a blood pressure measurement and a resting ECG, both of which had to be normal. If there were any risk factors that could potentially reduce physical fitness, such as an acute viral/bacterial infection or ongoing antibiotic therapy, the subject was immediately excluded from participating in the course.

All human centrifuge runs in which participants suffered G-LOC during one of the above flight profiles were extracted from the complete database of GAFCAM (n = 169). Since individual course participants had suffered several G-LOCs while completing the various profiles as part of their course participation, only the first G-LOC suffered was used for further analysis in order to rule out any possible after-effects. As a result, 47 G-LOCs had to be excluded from further analysis. Furthermore, all course participants for whom complete physiological data was no longer available were excluded (n = 36). This meant that a total of 86 G-LOC cases could be included in the evaluation (=G-LOC group).

For each of these cases, a course participant was identified who was matched in terms of age, nationality, training type and anti-G equipment and who had not suffered G-LOC during their training run (=control group).

The average age of the G-LOC group was 24.7 ± 3.7 years, with a body weight of 79.6 ± 9.4 kg and a height of 180.9 ± 5.8 cm (body mass index: 24.3 ± 2.4 kg/m^2). The participants in this group suffered a G-LOC during an LP without AGSM (n = 3 [3%]), LP with AGSM (n = 17 [20%]), Active I (n = 14 [16%]) and Active II (n = 52 [60%]) flight profiles. Due to the multinationality of the course participants, the test subjects came from different countries of origin. A 1:1 match was made in terms of flight profile and country of origin; in terms of age and anthropometric data, the G-LOC group did not differ significantly from the control group (see Table 1).

The physiological data and +G_z acceleration data for each participant were exported from the human centrifuge control programme and transferred to a Microsoft® Excel® (Microsoft, Albuquerque, NM, USA) spreadsheet. A computer algorithm was used to automatically detect pulse wave intervals and amplitudes (see Figure 3).

In order to analyse pulse wave flattening using the algorithm, three reference values were defined and calculated for each centrifuge run:

(1) An average value of the heights from 30 pulse wave curves at the start of the human centrifuge run at +1.4 Gz (hereinafter referred to as reference$_{n=30}$);

(2) The mean value of all pulse wave heights over the entire centrifuge run (referred to as reference$_{average}$); and
(3) The median of all pulse wave heights over the entire centrifuge run (referred to as the reference$_{median}$).

Table 1. Comparison of data from course participants who suffered G-LOC with that from the matched control group; nations were anonymised for security reasons; AGSM = anti-G straining manoeuvre.

	G-LOC Group	Control Group	*p*
n	86	86	
Centrifuge Profile			
- LP without AGSM	3	3	
- LP with AGSM	17	17	
- Active I	14	14	
- Active II	52	52	
Nations			
- Number 1	14	14	
- Number 2	41	41	
- Number 3	6	6	
- Number 4	1	1	
- Number 5	9	9	
- Number 6	2	2	
- Number 7	5	5	
- Number 8	4	4	
- Number 9	1	1	
- Number 10	4	4	
Age [years]	24.7 ± 3.7	24.3 ± 4.0	0.353
Weight [kg]	79.6 ± 9.4	79.6 ± 8.0	0.986
Size [cm]	180.9 ± 5.8	179.5 ± 5.2	0.103
BMI [kg/m^2]	24.3 ± 2.4	24.7 ± 2.2	0.215

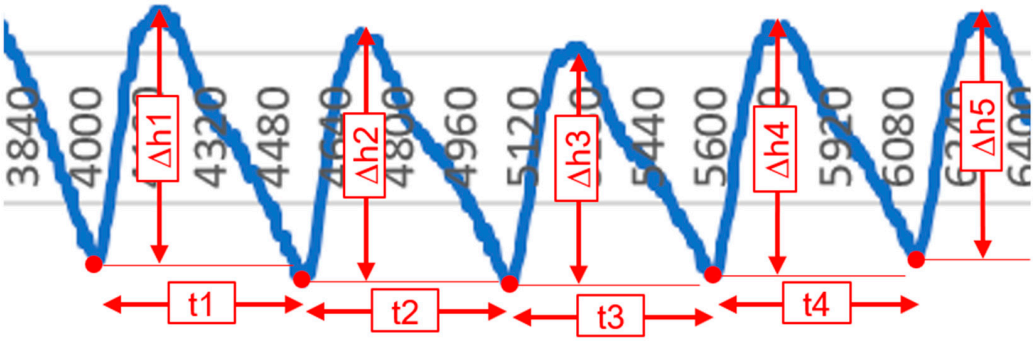


Figure 3. Automated detection of pulse waves using an algorithm and calculation of time intervals (t1–t4) and pulse wave heights (Δh1–Δh4). The figures shown in the diagram represent the timestamp of the human centrifuge run.

Each individual pulse wave was then analysed by the algorithm in relation to these three reference values, and the percentage ratio to the three reference values was calculated. If the individual pulse wave was below a threshold value of 90% (and then in 10%

increments down to 20%) of the respective reference value, the pulse wave flattening was assumed to be present, whereby the time durations were added together for successive pulse waves that each showed a corresponding reduction in pulse wave height below the cut-off value. This means that, for example, if three consecutive pulse waves were below the reference value, the time intervals of these three pulse waves were added together to obtain the total duration, in seconds, during which the pulse wave was below the reference value at that point. Thus, eight analyses were performed for each centrifuge run and for each of the three reference values (<90% to <20%). Assuming that reduced blood flow is associated with G-LOC, the length of the pulse wave flattening (in ms) was evaluated depending on the G-LOC event in the G-LOC group (all other pulse wave flattening events before and after the G-LOC were ignored). The exact time of G-LOC was determined for each of the subjects in the G-LOC group based on video analysis. In the control group, the longest pulse wave flattening (in ms) during the entire human centrifuge run was used for further analysis. An overall flow-chart of the analysis is shown in Figure 4.

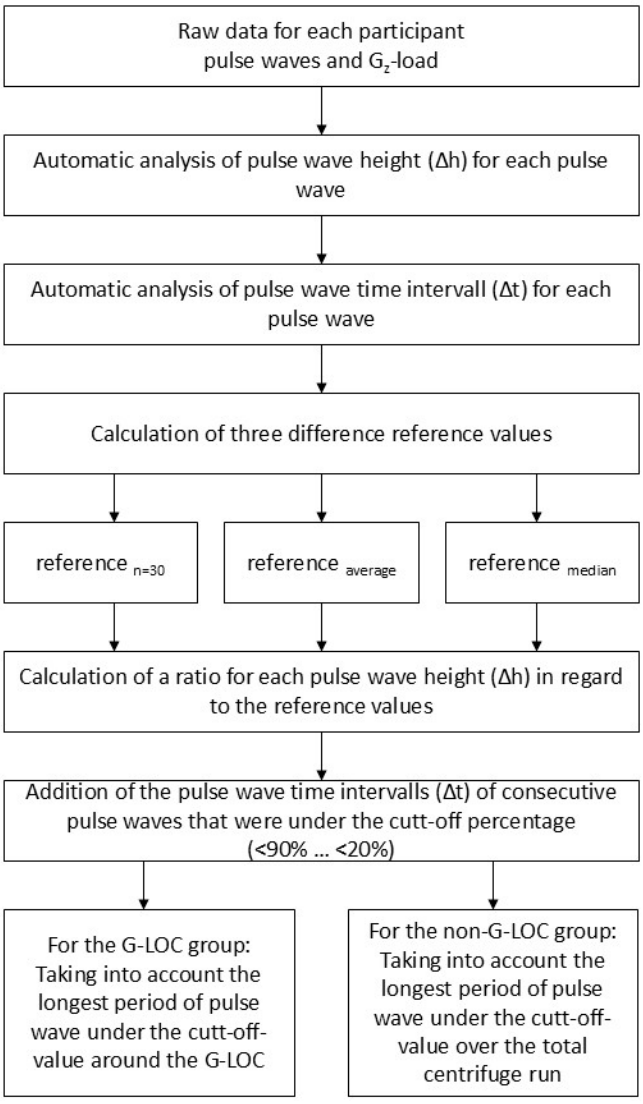


Figure 4. Flow-chart of the different steps of the automatic analysis.

The analysis was performed once for all profiles together and separately for the respective profiles, once for the active profiles, where the pilots themselves were allowed to determine the onset (Active I: n = 14 and Active II: n = 52), and once for the LP with AGSM

(n = 17). Since only three subjects in the LP without AGSM had suffered G-LOC, this was not evaluated separately.

Statistical analysis was performed using IBM SPSS Statistics 24 (IBM, Armonk, NY, USA). All parameters are shown as mean with standard deviation or as median with minimum and maximum. Due to non-normally distributed data, which was determined according to the Kolmogorov–Smirnov test for all parameters that measured the pulse wave deviation, the comparison for each reference value and each cut-off value was performed using the Wilcoxon signed-rank test for paired samples. The significance level was set at $p < 0.05$.

This study is part of the departmental research activity of the GAFCAM. No additional medical, diagnostic or therapeutic measures were carried out for the analysis, and no formal approval is required for the purely retrospective analysis in accordance with the specifications of the responsible ethics committee of the State Chamber of Physicians of Saxony (Az EK-BR-108/24-1).

3. Results

In the analysis of pulse wave flattening, the control group showed significantly longer phases of pulse wave flattening than the G-LOC group for all three reference values at minor pulse wave flattening (<70% to <90%), while at a stricter cut-off value (equivalent to a lower percentage of the reference value), there was no longer a significant difference between the two groups (see Table 2).

Table 2. Comparison of pulse wave flattening duration in the G-LOC group compared to the control group with anthropometric data; independent of flight profile (n = 86). All values for pulse wave flattening are shown as median [minimum–maximum]. Significant results are highlighted in bold.

All	G-LOC Group	Control Group	p
n	86	86	
Pulse wave flattening with reference$_{n=30}$ (only around the G-LOC)			
- 90% [ms]	6333 [720–311,170]	10,323 [1000–133,105]	**<0.001**
- 80% [ms]	5645 [720–311,170]	8003 [985–133,105]	**0.011**
- 70% [ms]	5338 [610–311,170]	6275 [865–133,105]	0.058
- 60% [ms]	4603 [535–311,170]	4583 [665–133,105]	0.268
- 50% [ms]	4260 [330–311,170]	3593 [665–133,105]	0.485
- 40% [ms]	3510 [325–311,170]	2670 [475–133,105]	0.360
- 30% [ms]	2785 [325–311,170]	2230 [450–133,105]	0.264
- 20% [ms]	1685 [330–311,170]	1613 [355–133,105]	0.287
Pulse wave flattening with reference$_{average}$ (only around the G-LOC)			
- 90% [ms]	6738 [930–260,330]	16,400 [2370–133,105]	**<0.001**
- 80% [ms]	5740 [720–260,330]	10,488 [1700–133,105]	**<0.001**
- 70% [ms]	5193 [720–260,330]	8305 [985–133,105]	**0.001**
- 60% [ms]	4603 [720–245,895]	5481 [865–133,105]	0.294
- 50% [ms]	3928 [330–245,895]	4330 [680–133,105]	0.818
- 40% [ms]	2925 [330–245,895]	3288 [680–133,105]	0.943
- 30% [ms]	2755 [330–88,575]	2285 [475–133,105]	0.242
- 20% [ms]	1940 [325–88,575]	1723 [355–133,105]	0.114

Table 2. *Cont.*

All	G-LOC Group	Control Group	*p*
Pulse wave flattening with reference$_{median}$ (only around the G-LOC)			
- 90% [ms]	5740 [420–27,100]	10,978 [1410–105,405]	**<0.001**
- 80% [ms]	5248 [330–27,100]	8298 [1300–105,405]	**<0.001**
- 70% [ms]	4468 [330–26,900]	6303 [950–105,405]	**0.008**
- 60% [ms]	4073 [330–26,900]	4402 [585–42,835]	0.318
- 50% [ms]	2898 [200–26,900]	3105 [445–41,955]	0.830
- 40% [ms]	2798 [170–25,905]	2570 [445–30,185]	0.991
- 30% [ms]	2083 [75–14,515]	1830 [445–19,520]	0.811
- 20% [ms]	1513 [75–13,410]	1523 [290–14,520]	0.697

The comparison of the subjects in the sub-analysis with active profiles up to +9 G_z (Active II) also showed no group differences in terms of age, weight, and height between the two groups (see Table 3). Here, too, the analysis of pulse wave flattening for the control group showed significantly longer phases of this pulse wave flattening for all three reference values than in the G-LOC group, which in some cases reached a cut-off value of <50%. With stricter cut-off values, there was no longer a significant difference between the two groups (see Table 3), but the duration of pulse wave flattening tended to be longer in the control group.

Table 3. Comparison of pulse wave flattening duration in the G-LOC group compared to the control group with anthropometric data; active performance profile up to +9 G_z (n = 52). All values for pulse wave flattening are shown as median [minimum–maximum] in ms. Significant results are highlighted in bold.

Active II	G-LOC Group	Control Group	*p*
n	52	52	
Age [years]	25.0 ± 4.7	24.5 ± 4.4	0.341
Weight [kg]	77.9 ± 9.2	80.3 ± 7.7	0.164
Size [cm]	181.1 ± 6.1	180.2 ± 4.8	0.390
BMI [kg/m^2]	23.7 ± 2.1	24.7 ± 2.1	**0.011**
Pulse wave flattening with reference$_{n=30}$ (only around the G-LOC)			
- 90% [ms]	5618 [720–21,475]	11,958 [1715–133,105]	**<0.001**
- 80% [ms]	5208 [720–21,115]	10,800 [1500–133,105]	**<0.001**
- 70% [ms]	4400 [610–17,775]	7797 [1100–133,105]	**0.001**
- 60% [ms]	4172 [535–17,695]	5138 [665–133,105]	**0.009**
- 50% [ms]	3745 [330–17,695]	4657 [665–133,105]	**0.031**
- 40% [ms]	2823 [325–17,695]	4724 [630–133,105]	0.312
- 30% [ms]	2328 [325–17,695]	3626 [545–133,105]	0.400
- 20% [ms]	1685 [325–10,580]	1625 [405–133,105]	0.604

Table 3. *Cont.*

Active II	G-LOC Group	Control Group	*p*
Pulse wave flattening with reference$_{average}$ (only around the G-LOC)			
- 90% [ms]	5405 [930–18,350]	16,600 [4565–133,105]	**<0.001**
- 80% [ms]	4923 [720–18,350]	11,438 [3240–133,105]	**<0.001**
- 70% [ms]	4468 [720–17,695]	8918 [2090–133,105]	**<0.001**
- 60% [ms]	4073 [720–17,695]	7308 [1300–133,105]	**0.004**
- 50% [ms]	3000 [330–17,695]	4585 [940–133,105]	**0.032**
- 40% [ms]	2758 [330–17,695]	3413 [940–133,105]	0.103
- 30% [ms]	2238 [330–17,695]	2318 [505–133,105]	0.566
- 20% [ms]	2306 [325–13,410]	1740 [410–133,105]	0.813
Pulse wave flattening with reference$_{median}$ (only around the G-LOC)			
- 90% [ms]	5338 [720–18,350]	11,118 [1410–105,405]	**<0.001**
- 80% [ms]	4795 [330–18,350]	8315 [1300–105,405]	**<0.001**
- 70% [ms]	4235 [330–17,695]	7403 [950–105,405]	**<0.001**
- 60% [ms]	2938 [330–17,695]	7643 [585–42,835]	**0.011**
- 50% [ms]	2823 [330–13,410]	3703 [445–41,955]	0.084
- 40% [ms]	3137 [330–13,410]	2605 [445–30,185]	0.265
- 30% [ms]	2030 [250–13,410]	2255 [445–19,520]	0.594
- 20% [ms]	1598 [250–13,410]	1605 [290–14,520]	0.827

When comparing the subjects in the sub-analysis with active profile up to +9 G_z (Active I), no group differences were found in terms of age, weight, and height between the two groups (see Table 4). Here, there were largely no significant differences between the two groups across all cut-off values and in relation to all reference values, although depending on the reference value used, the control group tended to show longer phases of pulse wave flattening (reference$_{average}$ and reference$_{median}$).

Table 4. Comparison of pulse wave flattening duration in the G-LOC group compared to the control group with anthropometric data; performance profile up to +7 G_z (n = 14). All values for pulse wave flattening are shown as median [minimum–maximum]. Significant results are highlighted in bold.

Active I	G-LOC Group	Control Group	*p*
n	14	14	
Age [years]	24.4 ± 1.9	24.3 ± 4.5	0.898
Weight [kg]	83.6 ± 10.3	78.6 ± 9.6	0.183
Size [cm]	182.1 ± 4.5	179.9 ± 6.1	0.271
BMI [kg/m^2]	25.2 ± 2.9	24.3 ± 2.6	0.337
Pulse wave flattening with reference$_{n=30}$ (only around the G-LOC)			
- 90% [ms]	8910 [1475–311,170]	8170 [3125–97,400]	0.594
- 80% [ms]	7833 [1455–311,170]	7043 [2765–97,400]	0.594
- 70% [ms]	5635 [1455–311,170]	6575 [1725–93,945]	0.433
- 60% [ms]	4238 [885–311,170]	5658 [885–93,945]	0.363
- 50% [ms]	3908 [885–311,170]	5273 [885–93,945]	0.510

Table 4. *Cont.*

Active I	G-LOC Group	Control Group	*p*
Pulse wave flattening with reference$_{n=30}$ (only around the G-LOC)			
- 40% [ms]	2428 [885–311,170]	4843 [765–91,950]	0.875
- 30% [ms]	2195 [885–311,170]	3385 [545–78,990]	0.975
- 20% [ms]	2035 [530–311,170]	4638 [545–76,010]	0.778
Pulse wave flattening with reference$_{average}$ (only around the G-LOC)			
- 90% [ms]	6525 [1580–260,330]	22,178 [6120–132,490]	0.074
- 80% [ms]	6130 [1580–260,330]	17,748 [4535–87,120]	0.084
- 70% [ms]	4433 [1475–260,330]	9373 [4180–85,925]	0.096
- 60% [ms]	4150 [1475–245,895]	6935 [2075–54,245]	0.300
- 50% [ms]	3023 [885–245,895]	5045 [980–43,450]	0.551
- 40% [ms]	2440 [885–245,895]	4085 [885–31,800]	0.433
- 30% [ms]	2313 [885–88,575]	3405 [765–21,990]	0.638
- 20% [ms]	1550 [885–88,575]	2750 [545–8195]	0.875
Pulse wave flattening with reference$_{median}$ (only around the G-LOC)			
- 90% [ms]	6065 [1250–24,700]	15,885 [3960–45,255]	0.022
- 80% [ms]	5300 [1180–18,485]	11,710 [3960–35,010]	0.035
- 70% [ms]	4118 [685–18,485]	7058 [2215–21,730]	0.245
- 60% [ms]	3170 [630–18,485]	4438 [1725–21,730]	0.470
- 50% [ms]	2230 [630–18,485]	2930 [1360–21,730]	0.683
- 40% [ms]	1960 [630–18,485]	2225 [885–11,035]	0.826
- 30% [ms]	1770 [335–8710]	1688 [765–9755]	0.730
- 20% [ms]	1475 [335–8440]	1423 [545–6270]	0.826

A comparison of the subjects evaluated in the LP sub-analysis with AGSM also failed to reveal any group differences in terms of age, weight, and height between the G-LOC group and the control group (see Table 5). In contrast to the other profiles, however, significantly longer phases of pulse wave flattening were observed in the G-LOC group compared to the control group at cut-off values of <60% to <20% or lower.

Table 5. Comparison of pulse wave flattening duration in the G-LOC group compared to the control group with anthropometric data; linear profile (LP) with anti-G straining manoeuvre (AGSM) (n = 17). All values for pulse wave flattening are shown as median [minimum–maximum]. Significant results are highlighted in bold.

LP with AGSM	G-LOC Group	Control Group	*p*
n	17	17	
Age [years]	24.3 ± 1.4	24.5 ± 1.7	0.387
Weight [kg]	82.6 ± 8.3	80.4 ± 6.4	0.334
Size [cm]	178.9 ± 6.1	178.4 ± 5.3	0.826
BMI [kg/m^2]	25.8 ± 2.0	25.3 ± 1.8	0.369

Table 5. *Cont.*

LP with AGSM	G-LOC Group	Control Group	*p*
Pulse wave flattening with reference$_{n=30}$ (only around the G-LOC)			
- 90% [ms]	11,505 [1480–27,100]	4680 [1000–57,050]	0.554
- 80% [ms]	11,300 [1480–27,100]	3840 [985–53,535]	0.149
- 70% [ms]	11,025 [745–26,900]	3810 [865–23,050]	0.068
- 60% [ms]	7665 [745–26,900]	2865 [680–19,365]	**0.035**
- 50% [ms]	7665 [745–26,900]	2710 [680–17,340]	**0.049**
- 40% [ms]	7665 [745–25,905]	2280 [475–10,625]	**0.007**
- 30% [ms]	3215 [745–16,705]	1745 [450–6445]	**0.005**
- 20% [ms]	1590 [220–16,705]	1075 [355–3930]	**0.049**
Pulse wave flattening with reference$_{average}$ (only around the G-LOC)			
- 90% [ms]	11,175 [1480–27,100]	9730 [2370–44,645]	0.586
- 80% [ms]	10,970 [1480–27,100]	7400 [1700–43,960]	0.795
- 70% [ms]	9775 [1480–27,100]	3840 [985–27,955]	0.136
- 60% [ms]	9775 [1480–27,100]	3375 [865–13,005]	**0.004**
- 50% [ms]	9065 [1480–26,900]	2725 [680–10,625]	**0.003**
- 40% [ms]	5715 [745–26,900]	2590 [680–10,625]	**0.011**
- 30% [ms]	3215 [745–25,905]	1745 [475–6445]	**0.004**
- 20% [ms]	2565 [420–9975]	1405 [335–3930]	**0.019**
Pulse wave flattening with reference$_{median}$ (only around the G-LOC)			
- 90% [ms]	9530 [420–27,100]	7770 [2855–32,120]	0.758
- 80% [ms]	9135 [420–27,100]	4680 [2370–19,365]	0.523
- 70% [ms]	8300 [345–26,900]	4100 [1700–18,790]	0.076
- 60% [ms]	7665 [345–26,900]	3375 [995–13,205]	**0.013**
- 50% [ms]	6880 [200–26,900]	2710 [680–13,005]	**0.011**
- 40% [ms]	3740 [170–25,905]	2050 [680–10,625]	0.068
- 30% [ms]	2780 [75–14,515]	1715 [475–10,625]	0.193
- 20% [ms]	1195 [75–8675]	1405 [355–4485]	0.619

4. Discussion

Based on 86 subjects who had suffered G-LOC during training in a human centrifuge and using an automatic computer algorithm, this study was able to show that gradual "onset run" centrifuge profiles using AGSM resulted in longer pulse wave flattening around the G-LOC in this G-LOC group compared to the matched control group. However, this could not be verified in human centrifuge runs with active flight profiles and higher onset rates. An analysis of pulse wave flattening independent of the flight profile shows no prolonged pulse wave flattening in the G-LOC group, meaning that the method used here would not be readily applicable for use in actual flight.

G-LOCs continue to pose a serious problem in modern aviation, especially when flying HPA. This makes it all the more important to develop reliable procedures for detecting either G-LOC itself or an imminent G-LOC, in order to prevent pilot incapacitation and ultimately avoid loss of both pilot and aircraft. On the one hand, a method should detect G-LOC cases as accurately as possible and with 100% reliability. On the other hand, it should

also have as few false positives as possible so as not to generate unnecessary frequent "false alarms" that could distract the HPA pilot from his actual flight task.

From a physiological point of view, a drop in oxygen saturation in the brain due to reduced cerebral perfusion in the context of increased $+G_z$ stress can generally be assumed, which may be accompanied by G-LOC. This was shown by using non-invasive cerebral regional oximetry measurements [4,10,12,21,22]. However, due to the high variability of the individual parameters in NIR spectroscopy, it was not possible to make a reliable prediction for G-LOC. Alternatively, the effects of reduced cerebral oxygen saturation during human centrifuge runs can also be determined using EEG [23].

The results presented here complement these findings, but an additional analysis method was used based on an automatic computer algorithm, which on the one hand makes pulse wave flattening machine-readable and thus also usable in aircraft, and on the other hand also enables a wider range of possible analyses of changes in pulse wave flattening. Even if such an approach were unable to detect G-LOC before it occurs, reliable detection during flight—enabling the computer to take over control automatically if necessary—would still offer a way of potentially saving both the pilot and the aircraft in future. These approaches are relatively new; they need more research and are not available at the moment. For example, Ohrui et al., in a study from 2024 [9], also use a machine learning algorithm based on a support vector machine to predict G-LOC in flight students during centrifuge runs using various variables such as cerebral oxyhaemoglobin and deoxyhaemoglobin concentrations. However, using the algorithm employed, G-LOC could only be predicted with an accuracy of 65% and 2.5 s after the onset of high $+G_z$ stress.

Algorithm-based methods have also been used for other physiological measurement methods to detect possible G-LOC. For example, the analysis of EMG measurements [20] was evaluated, but the predictive power of these methods was also insufficient.

The study presented here expands on previous findings in several respects. Firstly, a large number of G-LOCs were examined under different conditions and alternative approaches to evaluation were used with three different reference values in each case. The stepwise analysis with a cut-off value of <90% to <20% of the initial value also offers the possibility of a differentiated evaluation. Interestingly, on the one hand, training runs with a "gradual onset", i.e., a constant increase in $+G_z$ load, produced the expected effect of significantly longer pulse wave flattening in the G-LOC group. On the other hand, however, this was not the case with active flight profiles, as are regularly encountered in real flight. This can be explained by the fact that gradual centrifuge runs allow sufficient time for the cardiovascular system to activate and compensate for a rapid drop in regional cerebral oxygen supply, whereas in the case of short and possibly strong $+G_z$ changes, the drop in cerebral oxygen saturation is so severe that physiological compensation mechanisms cannot take effect in time before G-LOC occurs [21,22]. These rapid changes cannot therefore be detected in the pulse wave flattening, which is consistent with the results obtained here.

The study presented here has several strengths and limitations. One strength of the present study is the large sample size of 86 participants included in both the G-LOC group and the control group. Another strength is the 1:1 matched control group in terms of age, country of origin, training type and anti-G equipment, which also showed almost no significant differences in age, weight, height and BMI compared to the G-LOC group in the sub-analyses (with only one exception for BMI in the subgroup with Active II centrifuge profile).

Another strength is the machine-based algorithmic analysis of pulse wave height. This approach has several advantages over conventional methods: for example, pulse wave flattening was evaluated in a machine-readable format using machine recording, making this method independent of individual interpretation by human evaluators. Furthermore,

machine-readable evaluation has been taken into account for subsequent implementation in an automated system in the aircraft. In addition, this approach allowed for a wide range of different comparisons, both in terms of the choice of different reference values and the degree of pulse wave flattening, which significantly increased the scope of the evaluation carried out here. Furthermore, by analysing three different "flight profiles" in addition to a pure training run with increasing $+G_z$ loads, active flight profiles were also used to analyse more realistic $+G_z$ load changes. The differentiated results underline the importance of this approach.

However, it should also be noted as a limitation of the study that the analysis only used peripheral oxygen saturation with pulse wave display based on peripheral pulse oximetry. Other physiological parameters and measurement systems, such as heart rate, EMG or EEG, have not been analysed. However, this was not possible due to the retrospective methodological approach used in this study. Future analyses should therefore expand the automatic computer algorithms used here with machine learning methods to include such parameters and measurement methods, which should be evaluated individually or in combination.

This study was able to show that automatic computer algorithms could in some cases be used to analyse pulse wave flattening in peripheral pulse oximetry for the detection of G-LOC. The partially differing results, depending on which centrifuge profile was analysed, need to be further analysed. One possible solution here would be the (simultaneous) use of additional physiological measurement methods, which could make the detection or maybe also the prediction of G-LOC more probable.

5. Conclusions

In summary, based on the available results, pulse wave flattening alone cannot be used to detect a G-LOC under G_z loads. Future research efforts should therefore aim to expand the (physiological) data set in order to achieve at least reliable detection of G-LOC after it has occurred, which in turn would enable the automatic or remote takeover of the pilot's duties.

Author Contributions: Conceptualization, J.S., A.S. and S.S.; methodology, A.S. and S.S.; software, S.S.; validation, J.S. and S.S.; formal analysis, J.S. and S.S.; investigation, J.S. and M.N.; resources, M.N.; writing—original draft preparation, J.S.; writing—review and editing, A.S., M.N. and S.S.; visualisation, S.S.; supervision, S.S.; project administration, S.S. All authors have read and agreed to the published version of the manuscript.

Funding: This research received no external funding.

Data Availability Statement: The data associated with this study is not deposited into a publicly available repository. The data will be made available on request. The request must be addressed to the German Ministry of Defence.

Acknowledgments: We would like to thank the staff of the Aviation Physiology Training Centre in Königsbrück for providing the data and especially the former head of section for flight physiology research from this training centre for suggesting this study.

Conflicts of Interest: All authors are active Bundeswehr officers and work for the German Federal Ministry of Defence. All authors declare that the research was conducted in the absence of any commercial, financial, or non-financial relationships that could be construed as a potential conflict of interest. This article reflects the opinion of the authors only and not necessarily the opinions of the German Department of Defence or the Surgeon General of the German Air Force.

Abbreviations

The following abbreviations are used in this manuscript:

AGSM	anti-G straining manoeuvre
A-LOC	almost loss of consciousness
AP	acclimatisation profile
ECG	electrocardiogram
EEG	electroencephalography
EMG	electromyography
GAFCAM	German Air Force Centre of Aerospace Medicine
G-LOC	G-induced loss of consciousness
HPA	high-performance aircraft
LP	linear profile
NIRS	near-infrared spectroscopy
PBG	positive pressure breathing for G protection

References

1. Kim, S.; Nam, W.; Kil, H.; Park, M. Formal Verification of a Gravity-Induced Loss-of-Consciousness Monitoring System for Aircraft. *Comput. Sci. Eng.* **2014**, *16*, 96–103. [CrossRef]
2. Shaw, D.M.; Harrell, J.W. Integrating physiological monitoring systems in military aviation: A brief narrative review of its importance, opportunities, and risks. *Ergonomics* **2023**, *66*, 2242–2254. [CrossRef]
3. McKinley, R.A.; Tripp, L.D.; Bolia, S.D.; Roark, M.R. Computer modeling of acceleration effects on cerebral oxygen saturation. *Aviat. Space Environ. Med.* **2005**, *76*, 733–738.
4. Kurihara, K.; Kikukawa, A.; Kobayashi, A.; Nakadate, T. Frontal cortical oxygenation changes during gravity-induced loss of consciousness in humans: A near-infrared spatially resolved spectroscopic study. *J. Appl. Physiol.* **2007**, *103*, 1326–1331. [CrossRef] [PubMed]
5. Choi, H.S.; Sul, J.G.; Yi, K.S.; Seo, J.-M.; Chung, K.Y. Ultrasonographic finding of internal jugular vein during anti-G straining maneuver: Is it associated with gravity-induced loss of consciousness? *Eur. J. Appl. Physiol.* **2010**, *109*, 625–630. [CrossRef] [PubMed]
6. Whinnery, T.; Forster, E.M. The +Gz-induced loss of consciousness curve. *Extrem. Physiol. Med.* **2013**, *2*, 19. [CrossRef]
7. Shender, B.S.; Forster, E.M.; Hrebien, L.; Ryoo, H.C.; Cammarota, J.P. Acceleration-induced near-loss of consciousness: The "A-LOC" syndrome. *Aviat. Space Environ. Med.* **2003**, *74*, 1021–1028.
8. Copeland, K.; Whinnery, J.E. Cerebral Blood Flow Based Computer Modeling of Gz-Induced Effects. *Aerosp. Med. Hum. Perform.* **2023**, *94*, 409–414. [CrossRef]
9. Ohrui, N.; Iino, Y.; Kuramoto, K.; Kikukawa, A.; Okano, K.; Takada, K.; Tsujimoto, T. G-Induced Loss of Consciousness Prediction Using a Support Vector Machine. *Aerosp. Med. Hum. Perform.* **2024**, *95*, 29–36. [CrossRef]
10. Tripp, L.D.; Warm, J.S.; Matthews, G.; Chiu, P.Y.; Bracken, R.B. On Tracking the Course of Cerebral Oxygen Saturation and Pilot Performance During Gravity-Induced Loss of Consciousness. *Hum. Factors* **2009**, *51*, 775–784. [CrossRef] [PubMed]
11. Kim, S.; Choi, B.; Cho, T.; Lee, Y.; Koo, H.; Kim, D. Wearable bio signal monitoring system applied to aviation safety. *Annu. Int. Conf. IEEE Eng. Med. Biol. Soc.* **2017**, 2349–2352.
12. Tripp, L.D.; Warm, J.S.; Matthews, G.; Chiu, P.Y.; Bracken, R.B. Negative Acceleration and Adaptive Automation Approaches to Counter the Effect of Acceleration Induced Loss of Consciousness. *Proc. Hum. Factors Ergon. Soc. Annu. Meet.* **2008**, *52*, 1199–1203. [CrossRef]
13. Whinnery, A.M.; Whinnery, J.E.; Hickman, J.R. High+ Gz centrifuge training- The electrocardiographic response to+ Gz− induced loss of consciousness. *Aviat. Space Environ. Med.* **1990**, *61*, 609–614.
14. Tripp, L.D.; Warm, J.S.; Matthews, G.; Chiu, P.; Werchan, P.; Deaton, J.E. +Gz acceleration loss of consciousness: Time course of performance deficits with repeated experience. *Hum. Factors* **2006**, *48*, 109–120. [CrossRef]
15. Houghton, J.O.; McBride, D.K.; Hannah, K. Performance and Physiological Effects of Acceleration-Induced (+Gz). *Aviat. Space Environ. Med.* **1985**, *56*, 956–965.
16. Burton, R. G-induced loss of consciousness: Definition, history, current status. *Aviat. Space Environ. Med.* **1988**, *59*, 2–5.
17. Kim, C.; Koh, G. Integrated Flight Safety System to Cope with Gravity-Induced Loss of Consciousness—Industrial Perspective. *Int. J. Aeronaut. Space Sci.* **2025**, *26*, 1363–1385. [CrossRef]
18. Hrebien, L. Current and emerging technology in G-LOC detection: Pulse wave delay for+ Gz tolerance assessment. *Aviat. Space Environ. Med.* **1988**, *59*, 29–31. [PubMed]
19. Whinnery, T.; Forster, E.M. The first sign of loss of consciousness. *Physiol. Behav.* **2017**, *179*, 494–503. [CrossRef]

20. Li, Y.; Yang, J.; Li, B.; Jin, Z.; Zhang, L.; Yang, M. Investigation of early warning of EMG on human G-LOC under centrifuge high G load. *J. Phys. Conf. Ser.* **2024**, *2898*, 12003. [CrossRef]
21. Ryoo, H.C.; Sun, H.H.; Shender, B.S.; Hrebien, L. Consciousness monitoring using near-infrared spectroscopy (NIRS) during high +Gz exposures. *Med. Eng. Phys.* **2004**, *26*, 745–753. [CrossRef] [PubMed]
22. Ryoo, H.C.; Hrebien, L.; Shender, B.S. Noninvasive monitoring of human consciousness by near-infrared spectroscopy (NIRS) during high +Gz stress. *Biomed. Sci. Instrum.* **2002**, *38*, 1–7. [PubMed]
23. Wilson, G.F.; Reis, G.A.; Tripp, L.D. EEG correlates of G-induced loss of consciousness. *Aviat. Space Environ. Med.* **2005**, *76*, 19–27. [PubMed]

Disclaimer/Publisher's Note: The statements, opinions and data contained in all publications are solely those of the individual author(s) and contributor(s) and not of MDPI and/or the editor(s). MDPI and/or the editor(s) disclaim responsibility for any injury to people or property resulting from any ideas, methods, instructions or products referred to in the content.